Anomalous terahertz transmission through double-layer metal hole arrays by coupling of surface plasmon polaritons

Fumiaki Miyamaru* and Masanori Hangyo†
Institute of Laser Engineering, Osaka University, Yamadaoka 2-6, Suita, Osaka 565-0871, Japan
(Received 27 December 2004; published 7 April 2005)

The transmission characteristics of the double-layer metal hole array are investigated in the terahertz (THz) region. We measured the transmission spectra with varying the layer spacing and the lateral displacement between the two layers, and observed the unexpected transmission characteristics in the range of the layer spacing below the wavelength ($\lambda \sim 1$ mm) of the THz wave. When the second layer is shifted laterally by a half of the lattice constant with respect to the first layer, the transmittance is enhanced by 3 times compared with that without shift. The finite difference time domain simulation is used to understand this anomalous transmission phenomenon, and it is attributed to the near-field coupling of the surface waves excited on the metal surfaces of both layers.

DOI: 10.1103/PhysRevB.71.165408 PACS number(s): 78.66.Bz, 41.20.Jb, 42.79.Ci, 73.20.Mf

The optical property of the surface plasmon-polaritons (SPP's) has invoked a great deal of interest for many researchers because of their importance in physics and potential applications to engineering. The SPP's are localized at the metal-dielectric boundary, and the electric field of light is enhanced extremely. Recently, Ebbesen *et al.* demonstrated the extraordinary optical transmission through subwavelength metal hole arrays,[1] the diameters of which were much smaller than the wavelength of light. In their experiment, the metal hole array has bandpass transmission characteristics and the peak transmittance is about 2–3 times higher than the porosity of the hole. Up to now, such a bandpass transmission property has been investigated with many theoretical and experimental approaches and is attributed to the resonant coupling between the incident light and the SPP's excited on the metal-dielectric boundary through the periodic structure.[2–4] Although the frequency of the incident light is below the cutoff frequency of the metal hole, the reflectance is reduced by the resonant SPP excitation, and consequently, the transmittance of the metal hole array is enhanced. The above experiments are done with the samples for which the first-order diffraction frequency ν_{diff} determined by the lattice constant is lower than the cutoff frequency ν_{cutoff} of the single metal hole ($\nu_{\mathrm{diff}} < \nu_{\mathrm{cutoff}}$). In the THz region, it has been known that the transmission spectra of the metal hole arrays show bandpass characteristics and the peak transmittance is 2–3 times higher than the porosity for the case $\nu_{\mathrm{diff}} > \nu_{\mathrm{cutoff}}$ (Ref. 5). This enhanced transmission has also been interpreted by the SPP resonance.[6] However, in the THz region, metals are regarded as almost perfect conductors and most energy of the SPP's is owing to the electromagnetic wave localized at the air side. Thus, we call them surface waves (SW's) in this paper.

When the SPP's are excited on the two metal surfaces which are stacked with a separation closer than the attenuation length of the SPP's, the coupled states of the SPP's are constituted through the interaction between these SPP's.[7] Such a SPP coupling leads to new optical properties. By stacking some layers of the metal hole array, it is expected that the bandpass characteristic of the metal hole array due to the SPP excitation can be changed. In this paper, we investigate the transmission property of the double-layer metal hole arrays in the THz region and find the anomalous optical transmission property which is attributed to the near-field coupling between the SW's on the metal surfaces.

Figure 1(a) shows the schematic diagram of the double-layer metal hole array. Aluminum slabs were perforated with a triangular hole array. The transmission spectrum is characterized by three geometrical parameters such as a hole diameter ($d=0.60$ mm), lattice constant ($s=1.13$ mm), and thickness of the metal slab ($t=0.25$ mm). For this sample, the diffraction frequency is $\nu_{\mathrm{diff}}=0.31$ THz and the cutoff frequency is $\nu_{\mathrm{cutoff}}=0.29$ THz. In our experiment, the transmission characteristics were measured by using THz time-domain spectroscopy with varying the spacing h between the layers and the lateral displacement p which is along one of the principal axes of the triangular lattice. The details of the experimental setup are described in a previous paper.[8] The layer spacing h and the lateral displacement p were varied by a stepping motor-driven stage in the range between 0 and 2.0 mm.

Figure 1(b) shows the zero-order transmission spectrum for a single-layer metal hole array at normal incidence. The transmission peak is observed at 0.28 THz with a transmittance of 0.6, which is 2.3 times higher than the porosity of the circular holes (0.25). Such transmission peak is attributed to the resonant coupling of the incident THz wave to the SW's excited on the metal-air interface.[6]

The transmission spectra measured with varying the layer spacing at normal incidence are shown in Figs. 2(a) and 2(b) for $p=0$ and 0.57 mm, respectively. The schematics of configuration for the two layers are also shown in the insets of these figures. In both figures, stripe patterns are observed in the range $h>0.75$ mm and these patterns are similar for the two figures. Such stripe patterns are due to the Fabry-Perot effect between the two metal layers.[9] In the range of the layer spacing $h<0.75$ mm, the transmission spectra of the two configurations are quite different with each other. The transmission spectra at $h=0.35$ mm for two lateral displacements are shown in Fig. 2(c). The two spectra are quite different at

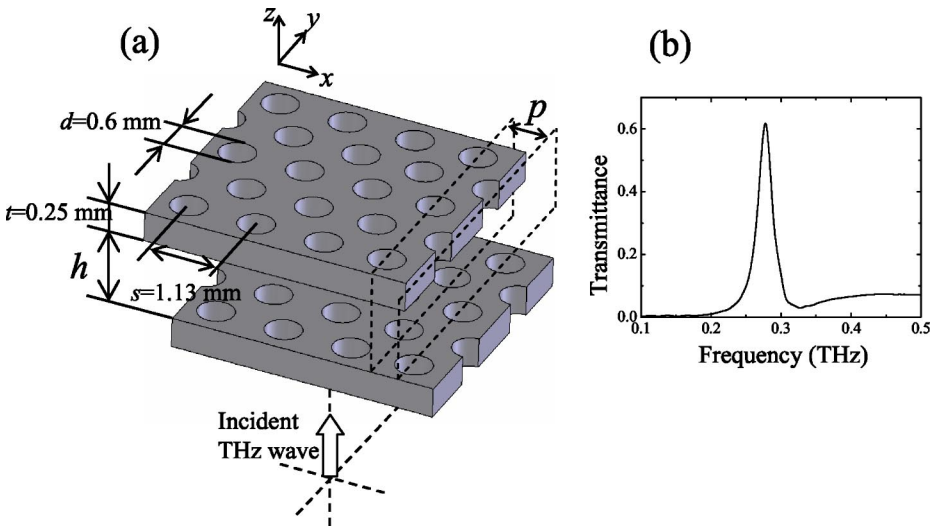

FIG. 1. (a) Schematic diagram of the double-layer metal hole array. (b) Measured transmission spectrum for the single-layer metal hole array.

$h=0.35$ mm while they are similar at $h=1.25$ mm [Fig. 2(d)]. Very interestingly, in Fig. 2(c), the peak transmittances at 0.26 and 0.28 THz for $p=0.57$ mm (solid line) are about 3 times higher than that at 0.27 and 0.29 THz for $p=0$ mm (dashed line). This result is unexpected from the geometrical configuration shown by the insets in Figs. 2(a) and 2(b). Since the conventional Fabry-Perot effect depends only on the layer spacing and is independent of the lateral displacement, the difference of the transmission spectra in Fig. 2(c) cannot be attributed to the Fabry-Perot effect between the two layers.

In order to investigate more details about the above results, we measured the dependence of the transmission spectra on the lateral displacement with the fixed layer spacing $h=0.35$ mm (Fig. 3). It is observed that the transmittance at the peak frequency increases with increasing the lateral displacement p from 0 to 0.57 mm. In addition, the transmission peak splits into a doublet and the splitting width becomes maximum at around $p=0.57$ mm. The transmittance at the peak frequency decreases with further increasing the lateral displacement and becomes minimum again at $p=1.13$ mm. There exists some asymmetry between both sides of the $p=0.57$ mm displacement, which is considered to be due to the misalignment of the sample setup.

Now we discuss the mechanism of such an anomalous transmission property for the double-layer metal hole array. In the visible region, the SPP is localized close to the metal surface and attenuated exponentially with going away from the metal surface. When the two layers of the metal hole array are placed closely, the SPP's excited on these layers couple with each other, and consequently, a change of the transmission spectrum is expected. To investigate the validity of this physical picture in the THz region, we simulated the electric field distribution for the single-layer metal hole array using the finite-difference time-domain (FDTD) method at first. The schematic diagram of the model used for the simulation is shown in Fig. 4(a). The simulation was done in a three-dimensional space with the periodic boundary condition along x and y directions, and the geometrical parameters of the single-layer metal hole array were the same with those

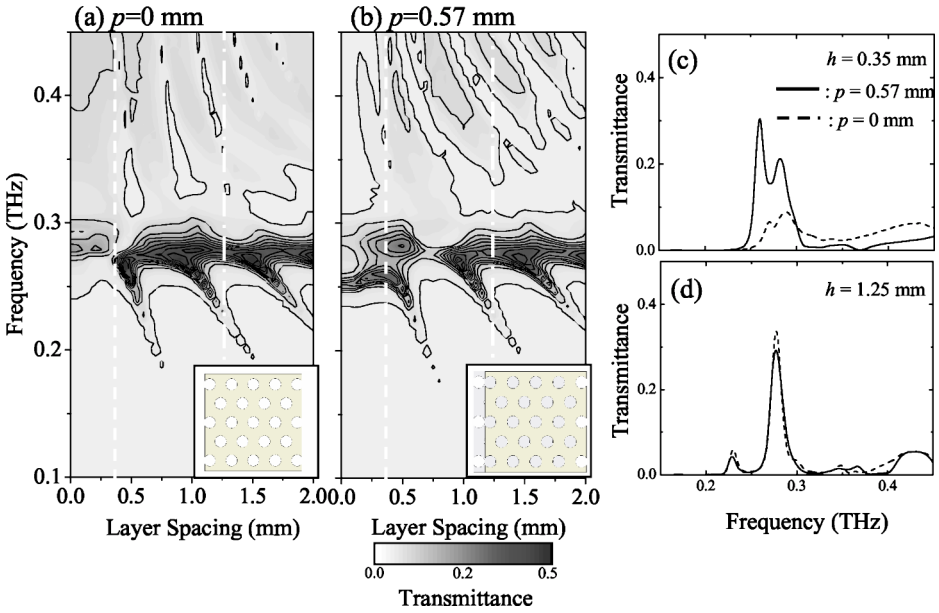

FIG. 2. Measured transmission spectra for the double-layer metal hole array as a function of the layer spacing ranging from 0 to 2.0 mm at (a) $p=0$ and (b) $p=0.57$ mm. Transmission spectra at the fixed layer spacing of (c) $h=0.35$ mm and (d) $h=1.25$ mm; solid and dashed lines are for $p=0.57$ and $p=0$ mm, respectively.

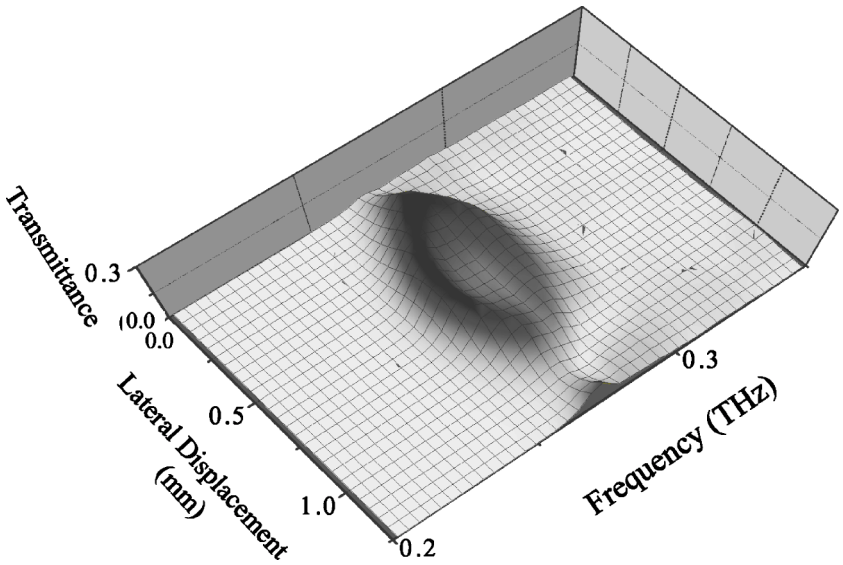

FIG. 3. Measured transmission spectra for the double-layer metal hole array as a function of the lateral displacement between the two layers at the fixed layer spacing $h=0.35$ mm.

of the sample used in our experiment. The metal part was assumed to be the perfect conductor. Since, for the THz wave, the real (ε_1) and imaginary (ε_2) parts of the dielectric constant of aluminum is of the order of $\varepsilon_1 \sim -50\,000$ and $\varepsilon_2 \sim 500\,000$, to consider the metal as the perfect conductor will be a good approximation. The incident THz wave was a plane wave with the linear polarization along the x axis, which is parallel to one of the principal axes of the triangular lattice structure. Figure 4(b) shows the calculated distribution of the z component E_z of the electric field amplitude at the resonant frequency of the SW. The electric field is concentrated around the edge of the circular hole and decays exponentially with going away from the metal surface, implying that the SW is excited. It should be noticed that on the flat surface of the metal, the attenuation length of the SPP in the air side becomes very large when the real part of the dielectric constant of the metal goes negative infinite, meaning the perfect conductor.[10] In this case, the SPP (or SW) does not exist. In the result of our simulation shown in Fig. 4(b), however, the strong localization of the electromagnetic wave is recognized and the attenuation length is on the order of the wavelength of incident electromagnetic waves even though the perfect conductor is used. Such an electromagnetic field distribution of the SW on the hole array of perfect conductors has also been reported by some groups.[11,12] Very recently, Pendry *et al.* reported the theoretical investigation about this issue.[13] In their theory, even for the perfect conductors the SW (or SW-like mode) exists when some kinds of structures such as hole arrays are fabricated. Such theoretical results support our simulated results of electromagnetic-wave localization at the metal surface. Figure 4(c) shows the amplitude of E_z (dotted line) along the dashed line in Fig. 4(b). The attenuation length into the air space, at which the field amplitude falls to $1/e$, is estimated to be 0.37 mm by fitting the calculated data to the exponential decay function (solid line). From this value, it is expected that the near-field coupling between the two SW's occurs in the range of $h<0.74$ mm. In Figs. 2(a) and 2(b), the anomalous transmission characteristics, which cannot be interpreted in terms of the Fabry-Perot effect, are observed only in the range of the layer spacing $h<0.75$ mm, which agree well with the above prediction. This result suggests that the anomalous transmission characteristics are attributed to the near-field coupling between the two SW's excited on the two layers. This near-field coupling leads to the splitting of the transmission peak as observed in Fig. 3. Recently, the tunability of the bandpass frequency by using the SPP coupling in the visible and near-infrared regions was reported by Wang.[14] He used the two metal-coated glass prisms which are separated by a narrow air gap. The transmission peak frequency was tuned in the range from 0.4 to 1.6 μm by changing the thickness of the air gap. In his case, SPP's were excited at the metal-air boundary using prism couplers and the coupled state between the two SW's depends on the spacing between two metal surfaces and is independent of the lateral displacement. In our experiment, however, the coupled state of the SPP's depends not only on the layer spacing but also on the lateral displacement owing to the periodic structure of the metal surface.

Figures 5(a) and 5(b) show the calculated distributions of the z component of the electric field amplitude at $p=0$ and $p=s/2$, respectively. The layer spacing is fixed in both figures at $h=0.35$ mm. The frequencies of the incident THz wave are 0.27 THz in Fig. 5(a) and 0.26 THz in Fig. 5(b), which are corresponding to the lower peak frequency observed in Fig. 2(c). In Fig. 5(a), the SW is excited on the surface of the first layer. At the output surface of the second layer, however, the SW is not excited, and the transmittance of the THz wave through the second layer holes becomes very low. In Fig. 5(b), on the other hand, it is observed that the SW's are excited on the surfaces of both first and second layers, and consequently, a higher transmittance is expected for $p=s/2$ in comparison with for $p=0$.

One question still remains for the transmission characteristic of the double-layer metal hole array. Why is the higher transmittance obtained for $p=s/2$ compared with for $p=0$? For the subwavelength metal aperture which is surrounded by circular periodic grooves, the high directivity of the emitted light from the output side of the metal film was observed recently.[15,16] The outgoing light at the resonant frequency of

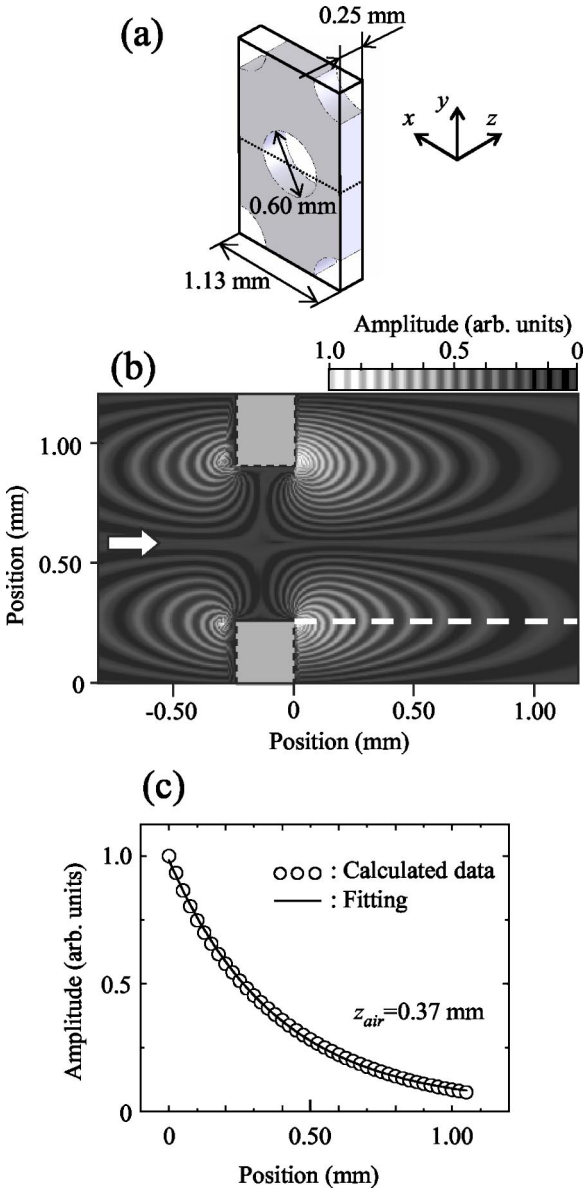

FIG. 4. (a) Schematic diagram of the model used in this simulation. (b) Simulated z component E_z of the electric field amplitude for the single-layer metal hole array. The cross section is taken along the one of the principal axes of the triangular lattice through the center of the hole. (c) The amplitude of E_z (dotted line) along the dashed line in Fig. 4(b) and the exponential fitting (solid line).

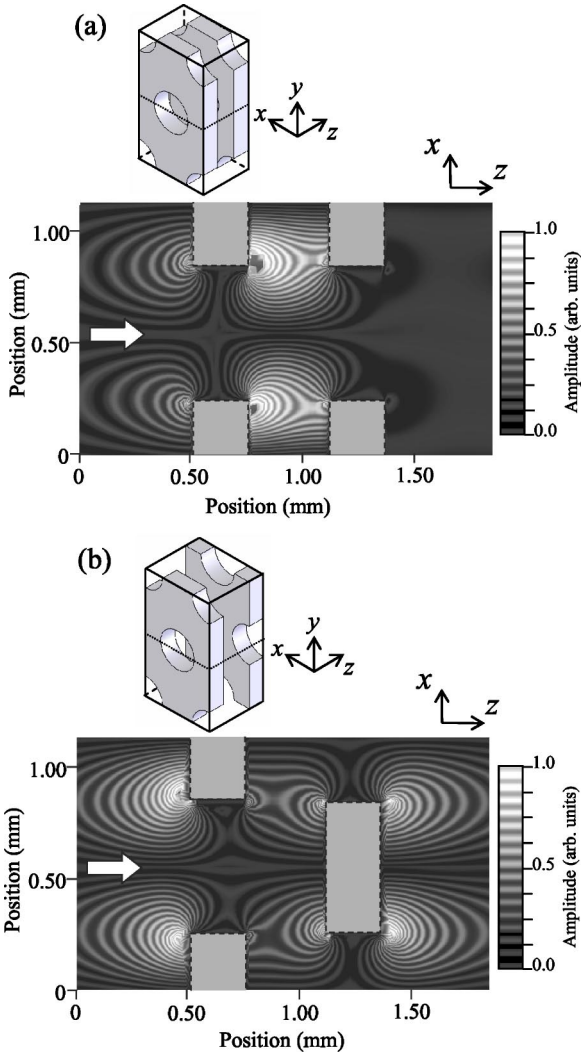

FIG. 5. Simulated z component E_z of the electric field amplitude for the double-layer metal hole array at (a) $p=0$ and (b) $p=s/2$ with the fixed layer spacing $h=0.35$ mm. The cross section is taken along the one of the principal axes of the triangular lattice through the center of the hole.

the SW at normal incidence is emitted to the zero-order direction which is perpendicular to the metal surface. Such a beaming effect of the transmitted light is also expected for the metal hole array studied in this paper. Thus, for the double-layer metal hole array, it is expected that most of the THz wave transmitted through the holes of the first layer would be blocked by the metal wall of the second layer for $p=s/2$. However, the results of our experiment [Fig. 2(c)] and the FDTD simulation (Fig. 5) are against such an expectation. To understand the origin of this phenomenon, we calculated the Poynting vector distribution for the single-layer metal hole array. Figure 6 shows the distribution of the Poynting vector simulated by the FDTD method for a single-layer metal hole array in the x-z plane. The simulation parameters are the same with those of Fig. 4(b). In Fig. 6, the THz wave enters from the bottom of the figure. The direction and length of arrows indicate the direction and intensity of the Poynting vector, respectively. The gray scale image indicates the intensity of the x component of the Poynting vector S_x and white and black colors mean positive and negative directions, respectively. It is observed that S_x is directed to the hole center at the input side, and on the other hand, it is directed away from the hole center at the output side. Such a Poynting vector distribution, which is caused by the SW, was reported by García-Vidal and Martin-Moreno for a metal slit array.[17] For the double-layer metal hole array, when the layer spacing is larger than the attenuation length of the SW's, the SW excited on each layers behaves independently and SW coupling does not occur. On the other hand, when the layer spacing is shorter than the attenuation length, the two SW's interact with each other and, as a result, new coupled states

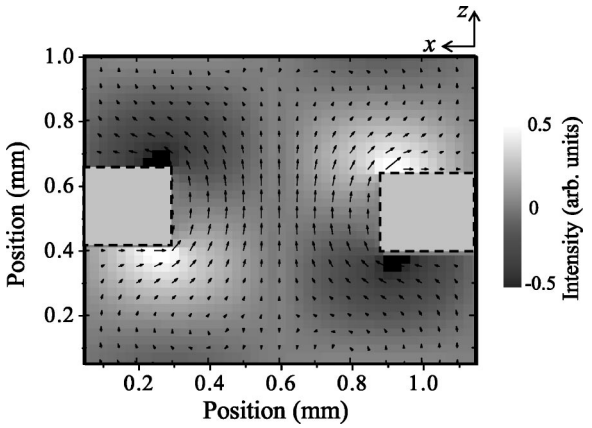

FIG. 6. Simulated Poynting vector for the single-layer metal hole array in the *x*-*z* plane (arrows). Gray scale image shows the intensity of the *x* component S_x of the Poynting vector. The cross section is taken along one of the principal axes of the triangular lattice through the center of the hole.

of the SW's are generated. In the case of $p=0$, where holes of the first and second layers are placed coaxially, destructive coupling of the two SW's is expected since the directions of S_x at the output side of the first layer and the input side of the second layer are opposite with each other. On the other hand, in the case of Fig. 5(b) ($p=s/2$), the direction of S_x at the output side of the first layer matches with that at the input side of the second layer. From this, it is concluded that the anomalous transmission characteristic for the double-layer metal hole array is attributed to the constructive coupling of the SW's for $p=s/2$ and destructive coupling for $p=0$.

In conclusion, we investigated the transmission characteristics of the double-layer metal hole array by varying the layer spacing and lateral displacement between the two layers. With increasing the layer spacing h, a typical change of the transmission spectrum corresponding to the Fabry-Perot effect is observed. In addition, an anomalous transmission characteristic is observed in the range of $h<0.75$ mm around the resonant frequency of the SW. The transmittance for lateral displacement of half the lattice constant is much higher than that without the displacement. From the result of the FDTD simulation, this anomalous transmission characteristic is attributed to the near-field coupling of the SW's which are excited on the output surface of the first layer and the input surface of the second layer. This phenomenon might make it possible to design a tunable filter or other optical devices not only in the THz region but also in the visible region. Further theoretical analysis would be needed for understanding the details of this phenomenon.

This work has been supported partly by the Grant-in-Aid for Scientific Research from the Ministry of Education, Culture, Sports, Science, and Technology, Japan.

*Electronic address: fmiyama@ile.osaka-u.ac.jp
†Electronic address: hangyo@ile.osaka-u.ac.jp

[1] T. W. Ebbesen, L. J. Lezec, H. F. Ghaemi, T. Thio, and P. A. Wolff, Nature (London) **391**, 667 (1998).
[2] L. Martín-Moreno, F. J. Garcia-Vidal, H. J. Lezec, K. M. Pellerin, T. Thio, J. B. Pendry, and T. W. Ebbesen, Phys. Rev. Lett. **86**, 1114 (2001).
[3] E. Popov, M. Nevière, S. Enoch and R. Reinisch, Phys. Rev. B **62**, 16100 (2000).
[4] W. L. Barnes, W. A. Murray, J. Dintinger, E. Devaux, and T. W. Ebbesen, Phys. Rev. Lett. **92**, 107401 (2004).
[5] C. Winnewisser, F. T. Lewen, M. Schall, M. Walther, and H. Helm, IEEE Trans. Microwave Theory Tech. **48**, 744 (2000).
[6] F. Miyamaru and M. Hangyo, Appl. Phys. Lett. **84**, 2742 (2004).
[7] G. J. Kovacs and G. D. Scott, Phys. Rev. B **16**, 1297 (1977).
[8] F. Miyamaru, T. Kondo, T. Nagashima, and M. Hangyo, Appl. Phys. Lett. **82**, 2568 (2003).
[9] K. Sakai, T. Fukui, Y. Tsunawaki, and H. Yoshinaga, Jpn. J. Appl. Phys. **8**, 1046 (1969).
[10] H. Raether, *Surface Plasmons on Smooth and Rough Surfaces and on Gratings* (Springer-Verlag, Berlin, 1988).
[11] J. Porto, F. J. García-Vidal, and J. B. Pendry, Phys. Rev. Lett. **83**, 2845 (1999).
[12] A. Krishnan, T. Thio, T. J. Kim, H. J. Lezec, T. W. Ebbesen, P. A. Wolff, J. Pendry, L. Martín-Moreno, and F. J. García-Vidal, Opt. Commun. **200**, 1 (2001).
[13] J. B. Pendry, L. Martín-Moreno, and F. J. García-Vidal, Science **305**, 847 (2004).
[14] Y. Wang, Appl. Phys. Lett. **82**, 4385 (2003).
[15] H. J. Lezec, A. Degiron, E. Devaux, R. A. Linke, L. Martín-Moreno, F. J. Garcíia-Vidal, and T. W. Ebbesen, Science **297**, 820 (2002).
[16] M. J. Lockyer, A. P. Hibbins, J. R. Sambles, and C. R. Lawrence, Appl. Phys. Lett. **84**, 2040 (2004).
[17] F. J. García-Vidal and L. Martín-Moreno, Phys. Rev. B **66**, 155412 (2002).